

Oscillating Casimir force between two slabs in a Fermi sea*

Chen Li-Wei(陈礼炜)^{a)}, Su Guo-Zhen(苏国珍)^{a)†},
Chen Jin-Can(陈金灿)^{a)}, and Andresen Bjarne^{b)}

^{a)}Department of Physics and Institute of Theoretical Physics and Astrophysics, Xiamen University, Xiamen 361005, China

^{b)}Niels Bohr Institute, University of Copenhagen, Universitetsparken 5, DK-2100 Copenhagen Ø, Denmark

(Received 28 June 2011; revised manuscript received 16 August 2011)

The Casimir effect for two parallel slabs immersed in an ideal Fermi sea is investigated at both zero and nonzero temperatures. It is found that the Casimir effect in a Fermi gas is distinctly different from that in an electromagnetic field or a massive Bose gas. In contrast to the familiar result that the Casimir force decreases monotonically with the increase of the separation L between two slabs in an electromagnetic field and a massive Bose gas, the Casimir force in a Fermi gas oscillates as a function of L . The Casimir force can be either attractive or repulsive, depending sensitively on the magnitude of L . In addition, it is found that the amplitude of the Casimir force in a Fermi gas decreases with the increase of the temperature, which also is contrary to the case in a Bose gas, since the bosonic Casimir force increases linearly with the increase of the temperature in the region $T < T_c$, where T_c is the critical temperature of the Bose–Einstein condensation.

Keywords: Casimir effect, Fermi gas, parallel slab, oscillation

PACS: 05.30.-d, 03.75.Ss, 05.30.Fk

DOI: 10.1088/1674-1056/21/1/010501

1. Introduction

The Casimir effect is an attractive interaction between two closely spaced parallel plates caused by the vacuum fluctuation of the electromagnetic field. About 10 years after its prediction in 1948 by Casimir,^[1] the Casimir force was measured experimentally by Spaarnay.^[2] More accurate measurement of the Casimir force was performed in a series of modern experiments^[3–7] starting with Lamoreaux’s landmark experiment in 1997.^[3] In theoretical developments, a great deal of effort has been devoted to the calculation of the Casimir energy or the Casimir force for different geometries and different boundary conditions,^[8–13] including those real structures of the boundaries. Its importance for practical applications is now becoming more widely appreciated in quantum field theory, Bose–Einstein condensates, atomic and molecular physics, gravitation and cosmology, and mathematical physics.

Generally, the presence of boundaries inside any wave field can cause Casimir-like effects if the bounded space is smaller than the maximum wavelength of the wave field. For example, an acoustic Casimir force

between two parallel rigid plates due to the radiation pressure of the band-limited acoustic noise was explored both theoretically and experimentally.^[14] Similarly, it may be expected that Casimir-like effects may occur in a quantum gas because of the wave character of the gas atoms. In Ref. [15], the Casimir force between two slabs immersed in a perfect Bose gas was calculated for various boundary conditions. It was found that the Casimir force has the standard asymptotic form with universal Casimir terms below the bulk critical temperature of Bose–Einstein condensation (BEC) T_c and vanishes exponentially above T_c . A question naturally comes to mind: what happens if the Bose gas is replaced by a Fermi gas?

The Casimir effect in fermionic fields has been extensively investigated in the literature. In this connection, a large amount of work has been devoted to the calculation of the Casimir interaction between two impurities or two bubbles immersed in a Fermi sea,^[16–18] which is particularly relevant to the physics of neutron stars^[19] and quark gluon plasmas.^[20] In most of those investigations, the Casimir force was calculated utilizing the geometry-dependent density of states,^[16,17]

*Project supported by the National Natural Science Foundation of China (Grant No. 10875100) and the Natural Science Foundation of Fujian Province, China (Grant No. A1010016).

†Corresponding author. E-mail: gzsx@xmu.edu.cn

© 2012 Chinese Physical Society and IOP Publishing Ltd

<http://iopscience.iop.org/cpb> <http://cpb.iphy.ac.cn>

in which the corrections arising from the presence of obstacles had been taken into account. As opposed to those previous studies, exact numerical calculations will be employed in the present paper to calculate the Casimir force between two slabs immersed in a Fermi sea.

2. Fermionic Casimir effect at zero temperature

We consider two large parallel slabs immersed in a sea of perfect Fermi gas. The two slabs are separated along the z axis by a small distance $L \ll \sqrt{A}$, where A is the area of the slab. The system of the fermions between the two slabs (confined system) is in thermodynamic equilibrium with the Fermi sea outside the slabs (surroundings). The single-particle energy of the confined system is given by

$$\varepsilon(\mathbf{k}) = \frac{\hbar^2}{2m}(k_x^2 + k_y^2 + k_z^2), \quad (1)$$

where m is the mass of the particle, \hbar is the reduced Planck constant and \mathbf{k} is the wave vector. For the problem under consideration, k_x and k_y are taken to be continuous, and k_z is quantized as

$$k_z = \frac{\pi n}{L}, \quad (2)$$

with $n = 1, 2, 3, \dots$ for the Dirichlet boundary condition (DBC), $n = 0, 1, 2, \dots$ for the Neumann boundary condition (NBC), and $n = 0, \pm 2, \pm 4, \dots$ for the periodic boundary condition (PBC).

We first consider the case at zero temperature ($T = 0$ K). The thermodynamic potential of the ideal Fermi gas at 0 K is given by

$$\Omega = - \sum_{\mathbf{k}} [\varepsilon_{\text{F}} - \varepsilon(\mathbf{k})] \theta(\varepsilon_{\text{F}} - \varepsilon(\mathbf{k})), \quad (3)$$

and can be derived as

$$\Omega = \begin{cases} -\frac{Ak_{\text{F}}^2\varepsilon_{\text{F}}}{8\pi} \sum_{n=1,0}^{J_1} \left[1 - \left(\frac{\pi n}{k_{\text{F}}L} \right)^2 \right]^2, & \text{for DBC and NBC,} \\ -\frac{Ak_{\text{F}}^2\varepsilon_{\text{F}}}{8\pi} \sum_{n=-J_2}^{J_2} \left[1 - \left(\frac{2\pi n}{k_{\text{F}}L} \right)^2 \right]^2, & \text{for PBC,} \end{cases} \quad (4)$$

where k_{B} is the Boltzman constant, ε_{F} is the Fermi energy of the confined system, which is equal to that of the surroundings in the state of equilibrium, $k_{\text{F}} = \sqrt{2m\varepsilon_{\text{F}}}/\hbar$, J_1 and J_2 are the integer parts of $k_{\text{F}}L/\pi$ and $k_{\text{F}}L/(2\pi)$, respectively, and the summation $\sum_{n=1,0}^{J_1}$ starts from 1 for DBC and 0 for NBC. The degeneracy related to the internal structure of the particles is assumed to be one for simplicity. From Eq. (4), the Casimir force per unit area can be derived as

$$P_{\text{C}}(L) = -\frac{1}{A} \left[\left(\frac{\partial \Omega}{\partial L} \right)_{\varepsilon_{\text{F}}, A} - \lim_{L \rightarrow \infty} \left(\frac{\partial \Omega}{\partial L} \right)_{\varepsilon_{\text{F}}, A} \right] \\ = \begin{cases} \left\{ \frac{\pi \varepsilon_{\text{F}}}{2L^3} \left\{ \sum_{n=1,0}^{J_1} n^2 \left[1 - \left(\frac{\pi n}{k_{\text{F}}L} \right)^2 \right] - \frac{2}{15} \left(\frac{k_{\text{F}}L}{\pi} \right)^3 \right\} \right\}, & \text{for DBC and NBC,} \\ \left\{ \frac{\pi \varepsilon_{\text{F}}}{2L^3} \left\{ \sum_{n=-J_2}^{J_2} (2n)^2 \left[1 - \left(\frac{2\pi n}{k_{\text{F}}L} \right)^2 \right] - \frac{2}{15} \left(\frac{k_{\text{F}}L}{\pi} \right)^3 \right\} \right\}, & \text{for PBC.} \end{cases} \quad (5)$$

Based on Eq. (5), we can understand the dependence of the Casimir force on the separation of the two slabs. For example, in the case of DBC, the scaled Casimir pressure can be directly derived from Eq. (5) to be

$$\frac{P_{\text{C}}}{P_{\text{S0}}} = \frac{5}{2} \frac{J_1(J_1 + 1/2)(J_1 + 1)}{(k_{\text{F}}L/\pi)^3} \\ \times \left[1 - \frac{3J_1^2 + 3J_1 - 1}{5(k_{\text{F}}L/\pi)^2} \right] - 1, \quad (6)$$

where P_{S0} is the pressure of the surroundings at 0 K and is given by $P_{\text{S0}} = \varepsilon_{\text{F}}k_{\text{F}}^3/(15\pi^2)$.^[21] In Eq. (6), the numerators contain J_1 and thus remain constants over each integer interval, while the denominators contain $(k_{\text{F}}L/\pi)^3$ and $(k_{\text{F}}L/\pi)^2$ and increase as $k_{\text{F}}L/\pi$ increases. For $k_{\text{F}}L/\pi < 1$, $J_1 = 0$ and $P_{\text{C}}/P_{\text{S0}} = -1$, which means that the Casimir force per unit area is equal to the pressure of the surroundings. This re-

sult is expected. When $k_F L/\pi < 1$, the energy of the lowest level of the confined system $\varepsilon_0 = \pi^2 \hbar^2/(2mL^2)$ is larger than the Fermi energy $\varepsilon_F = \hbar^2 k_F^2/(2m)$, so there will be no particle and hence no pressure in the space between the two slabs. For $k_F L/\pi \geq 1$, P_C/P_{S0} has a minimum

$$\frac{P_{C, \min}}{P_{S0}} = -\frac{5J_1^2 - 1}{4J_1^4} \quad (7)$$

at $k_F L/\pi = J_1$ ($J_1 = 1, 2, 3, \dots$) and a maximum

$$\frac{P_{C, \max}}{P_{S0}} = \frac{J_1(J_1 + 1/2)(J_1 + 1)}{(J_1^2 + J_1 - 1/3)^{3/2}} - 1 \quad (8)$$

at $k_F L/\pi = \sqrt{J_1^2 + J_1 - 1/3}$ in each integer interval from J_1 to $J_1 + 1$. Thus, P_C/P_{S0} as a function of $k_F L/\pi$ will oscillate with the period of $\Delta(k_F L/\pi) = 1$, as shown in Fig. 1. The property is not seen in the case of an electromagnetic field or a massive Bose gas, where the Casimir force is known to be a monotonically decreasing function of L . In each integer interval $J_1 \leq k_F L/\pi < J_1 + 1$, P_C/P_{S0} may vary between $P_{C, \min}/P_{S0} < 0$ and $P_{C, \max}/P_{S0} > 0$. It indicates that the Casimir force can be attractive or repulsive, alternating periodically with the increase of the separation between the two slabs. This gives rise to another important difference in the Casimir effects between the Bose and the Fermi gases, as the Casimir force for the former can only be attractive.^[15]

In the cases of NBC and PBC, the dependence of the Casimir force on the separation between the two slabs can be similarly discussed. It is found that the

curve of P_C/P_{S0} versus $k_F L/\pi$ in the case of NBC is the same as that in the case of DBC, while in the case of PBC, P_C/P_{S0} oscillates as a function of $k_F L/\pi$ with a doubled period, as shown in Fig. 1.

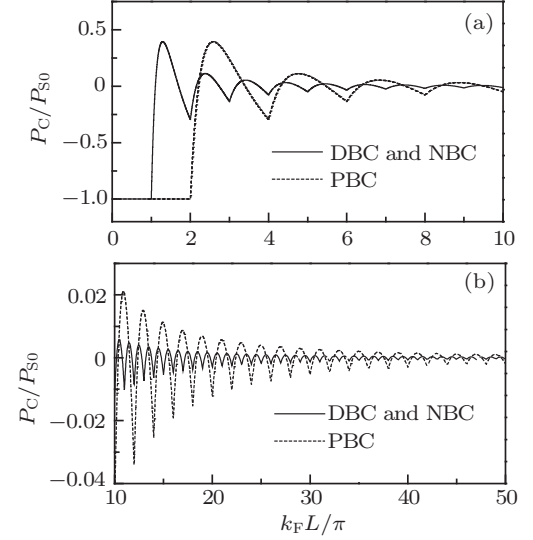


Fig. 1. Casimir forces versus separation between the two bounding slabs for different boundary conditions at zero temperature. Panels (a) and (b) give the results at small and large separations, respectively.

It is important to note that the particle density of the confined system is generally different from that of the surroundings when they are in thermodynamic equilibrium at constant temperature and chemical potential. According to Eq. (4), the difference in particle density between the confined system and the surroundings can be obtained as

$$\begin{aligned} \Delta\rho(L) &= -\frac{1}{A} \left[\frac{1}{L} \left(\frac{\partial\Omega}{\partial\varepsilon_F} \right)_{A,L} - \lim_{L \rightarrow \infty} \frac{1}{L} \left(\frac{\partial\Omega}{\partial\varepsilon_F} \right)_{A,L} \right] \\ &= \begin{cases} \frac{k_F^2}{4\pi L} \left\{ \sum_{n=1,0}^{J_1} \left[1 - \left(\frac{\pi n}{k_F L} \right)^2 \right] - \frac{2}{3} \left(\frac{k_F L}{\pi} \right) \right\}, & \text{for DBC and NBC,} \\ \frac{k_F^2}{4\pi L} \left\{ \sum_{n=-J_2}^{J_2} \left[1 - \left(\frac{2\pi n}{k_F L} \right)^2 \right] - \frac{2}{3} \left(\frac{k_F L}{\pi} \right) \right\}, & \text{for PBC.} \end{cases} \end{aligned} \quad (9)$$

By using Eq. (9), the curves of $\Delta\rho/\rho_{S0}$ versus $k_F L/\pi$ for different boundary conditions can be plotted, as shown in Fig. 2, where ρ_{S0} is the particle density of the surroundings at 0 K and is given by $\rho_{S0} = k_F^3/(6\pi^2)$.^[21] It is found that the curves each display a sawtooth-like oscillation that becomes smoother as

L increases. The values of $\Delta\rho/\rho_{S0}$ are sensitive to the boundary conditions: $\Delta\rho/\rho_{S0}$ is negative for DBC, positive for NBC, and varies alternately from positive to negative for PBC. When $L \rightarrow 0$, $\Delta\rho/\rho_{S0} = -1$ for DBC, and $\Delta\rho/\rho_{S0} \rightarrow \infty$ for NBC and PBC.

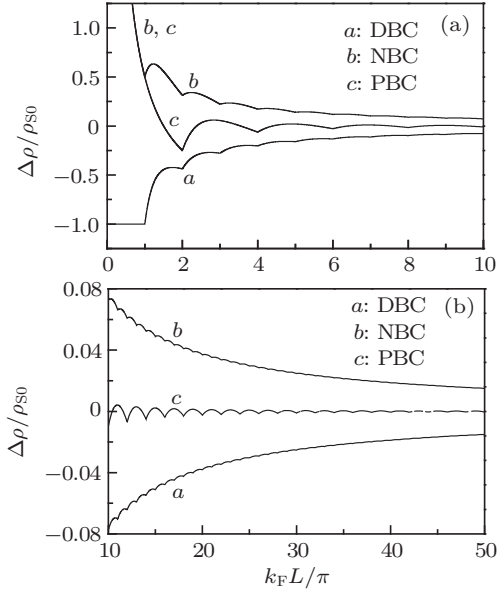


Fig. 2. Difference between the density of fermions between the two slabs and that outside the two slabs versus separation of the slabs for different boundary conditions at zero temperature. Panels (a) and (b) give the results at small and large separations, respectively.

3. Fermionic Casimir effect at nonzero temperatures

We now turn to the cases of nonzero temperatures and first consider the case of the Dirichlet boundary condition, for which the thermodynamic potential of the confined system at nonzero temperatures can be expressed as

$$\begin{aligned} \Omega &= -k_B T \sum_{\mathbf{k}} \ln[1 + z e^{-\beta \varepsilon(\mathbf{k})}] \\ &= -\frac{A k_T^2 k_B T}{4\pi} \sum_{n=1}^{\infty} f_2 \left(z \exp \left[-\left(\frac{\pi n}{k_T L} \right)^2 \right] \right), \end{aligned} \quad (10)$$

where $k_T = \sqrt{2mk_B T}/\hbar$, $z = e^{\mu/(k_B T)}$ is the fugacity, μ is the chemical potential of the confined system, which is equal to that of the surroundings in the state of equilibrium, $f_\nu(x)$ is the Fermi integral

$$f_\nu(x) = \frac{1}{\Gamma(\nu)} \int_0^\infty \frac{t^{\nu-1} dt}{x^{-1} e^t + 1}, \quad (11)$$

and $\Gamma(x)$ is the Gamma function. According to Eq. (10), we can find the Casimir force per unit area and the difference in particle density between the confined system and the surroundings to be

$$\begin{aligned} P_C(L, T) &= \frac{\pi k_B T}{2L^3} \left[\sum_{n=1}^{\infty} n^2 f_1 \left(z \exp \left[-\left(\frac{\pi n}{k_T L} \right)^2 \right] \right) \right. \\ &\quad \left. - \frac{\pi^{1/2}}{4} \left(\frac{k_T L}{\pi} \right)^3 f_{5/2}(z) \right] \end{aligned} \quad (12)$$

and

$$\begin{aligned} \Delta\rho(L, T) &= \frac{k_T^2}{4\pi L} \left[\sum_{n=1}^{\infty} f_1 \left(z \exp \left[-\left(\frac{\pi n}{k_T L} \right)^2 \right] \right) \right. \\ &\quad \left. - \frac{\pi^{1/2}}{2} \frac{k_T L}{\pi} f_{3/2}(z) \right], \end{aligned} \quad (13)$$

respectively, where the fugacity z is determined by

$$f_{3/2}(z) = \left(\frac{T_F}{T} \right)^{3/2} \frac{4}{3\pi^{1/2}}, \quad (14)$$

and $T_F = \varepsilon_F/k_B$ is the Fermi temperature. The dependences of $P_C(L, T)$ and $\Delta\rho(L, T)$ on parameters L and T can be obtained from Eqs. (12)–(14) using a numerical calculation.

Figure 3 shows the curves of P_C/P_{S0} varying with $k_F L/\pi$ for different values of the scaled temperature T/T_F . It can be seen that the amplitude of P_C/P_{S0} decreases with the increasing temperature. This property is different from that for the Bose gas, in which the Casimir force increases linearly with the increase of the temperature in the region $T < T_c$.^[15] Compared with the case $T = 0$ K, the curves of P_C/P_{S0} versus $k_F L/\pi$ at nonzero temperatures become smooth due to thermal excitation.

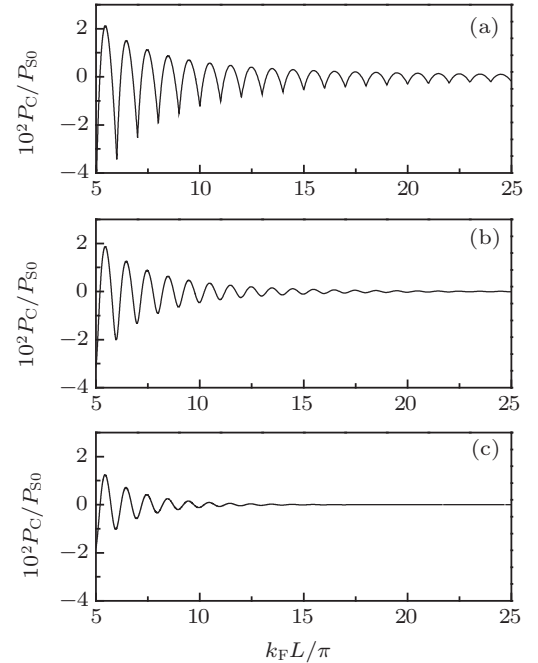


Fig. 3. Casimir force versus separation between the two slabs at (a) $T/T_F = 0$, (b) $T/T_F = 0.02$, and (c) $T/T_F = 0.04$.

Figure 4 shows the curves of P_C/P_{S0} varying with T/T_F for different values of parameter $k_F L/\pi$. It is observed that the curves can be significantly changed for a slight variation of $k_F L/\pi$. It indicates that the Casimir force is quite sensitive to the separation between the slabs.

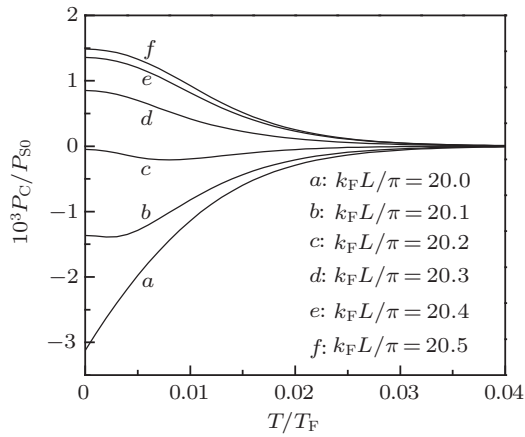


Fig. 4. Casimir force as a function of temperature for different separations between the slabs.

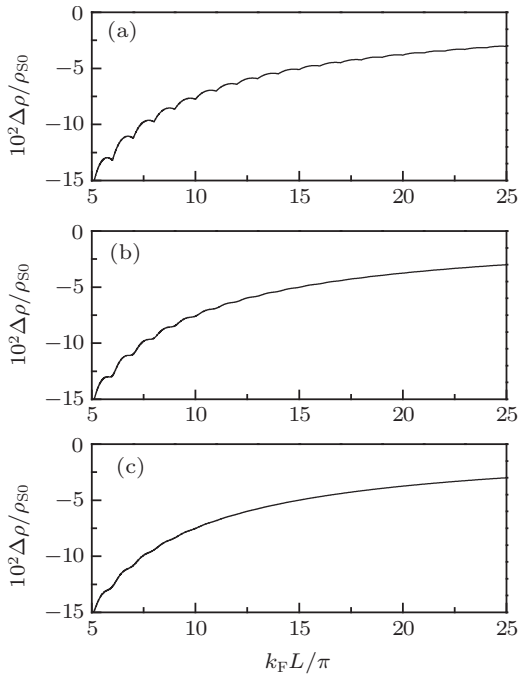


Fig. 5. Difference between the density of fermions between the two slabs and that outside the two slabs as a function of the separation of the slabs at (a) $T/T_F = 0$, (b) $T/T_F = 0.02$, and (c) $T/T_F = 0.04$.

Figure 5 gives the curves of $\Delta\rho/\rho_{S0}$ versus $k_F L/\pi$ for different values of parameter T/T_F , which are obtained using Eqs. (13) and (14). It can be seen that the oscillation of $\Delta\rho/\rho_{S0}$ with $k_F L/\pi$ gradually disappears with the increase of the temperature. In addition, it is found that for a given value of $k_F L/\pi$, the values of $\Delta\rho/\rho_{S0}$ are about the same for different values of T/T_F . This implies that the difference in particle density between the confined system and the surroundings is insensitive to the temperature in the low-temperature region.

The fermionic Casimir effects at nonzero temperatures are quite similar for the cases of NBC and PBC. Thus, they are not listed in detail here.

4. Conclusion

We study the Casimir effect for two parallel slabs immersed in a sea of perfect fermions. Some important results obtained are as follows. (i) The Casimir force in the ideal Fermi gas oscillates with the increase of the separation between the two slabs, which is distinctly different from that in the case of an electromagnetic field or a massive Bose gas. (ii) The fermionic Casimir force can be either attractive or repulsive, which is another important difference in the Casimir effect between the Bose and the Fermi gases. (iii) The amplitude of the Casimir force decreases with the increase of the temperature. This is opposite to that for the Bose gas, in which the Casimir force increases linearly with the increase of the temperature in the region $T < T_c$. (iv) The difference in particle density between the confined system and the surroundings is sensitive to the separation between the two slabs and the boundary conditions but is insensitive to the temperature in the low-temperature region.

References

- [1] Casimir H B G 1948 *Proc. Ned. Akad. Wet. B* **51** 793
- [2] Sparnaay M J 1958 *Physica* **24** 751
- [3] Lamoreaux S K 1997 *Phys. Rev. Lett.* **78** 5
- [4] Mohideen U and Roy A 1998 *Phys. Rev. Lett.* **81** 4549
- [5] Bressi G, Carugno G, Onofrio R and Ruoso G 2002 *Phys. Rev. Lett.* **88** 041804
- [6] Antonini P, Bressi G, Carugno G, Galeazzi G, Messineo G and Ruoso G 2006 *New J. Phys.* **8** 239
- [7] Petrov V, Petrov M, Bryksin V, Petter J and Tschudi T J 2007 *Exp. Theor. Phys.* **104** 96
- [8] Casadio R, Gruppiso A, Harms B and Micu O 2007 *Phys. Rev. D* **76** 025016
- [9] Zhai X H and Li X Z 2007 *Phys. Rev. D* **76** 047704
- [10] Alves D T and Granhen E R 2008 *Phys. Rev. A* **77** 015808
- [11] Lim S C and Teo L P 2009 *New J. Phys.* **11** 013055
- [12] Bai Z W 2004 *Acta Phys. Sin.* **53** 2472 (in Chinese)
- [13] Zeng R, Yang Y P and Liu S T 2008 *Acta Phys. Sin.* **57** 4947 (in Chinese)
- [14] Larraza B and Denardo B 1998 *Phys. Lett. A* **248** 151
- [15] Martin P A and Zagrebnov V A 2006 *Europhys. Lett.* **73** 15
- [16] Bulgac A and Wirzba A 2001 *Phys. Rev. Lett.* **87** 120404
- [17] Wirzba A, Bulgac A and Magierski P 2006 *J. Phys. A: Math. Gen.* **39** 6815
- [18] Recati A, Fuchs J N, Peça C S and Zwerger W 2005 *Phys. Rev. A* **72** 023616
- [19] Bulgac A and Magierski P 2001 *Nucl. Phys. A* **683** 695
- [20] Neergaard G and Madsen J 2000 *Phys. Rev. D* **62** 034005
- [21] Pathria R K 1972 *Statistical Mechanics* (2nd edn.) (Oxford: Pergamon Press) p. 198